Nontrivial Behavior of Water in the Vicinity and Inside Lipid Bilayers As Probed by Molecular Dynamics Simulations

Nikolay A. Krylov,[†,‡] **Vladimir M. Pentkovsky,**[§,⊥,||] **and Roman G. Efremov**[†,§,*]

[†]M.M. Shemyakin & Yu.A. Ovchinnikov Institute of Bioorganic Chemistry, Russian Academy of Sciences, ul. Miklukho-Maklaya, 16/10, Moscow 117997, Russia, [‡]Joint Supercomputer Center, Russian Academy of Sciences, Leninsky prospect, 32a, Moscow 119991, Russia, [§]Moscow Institute of Physics and Technology (State University), Institutskii per., 9, Dolgoprudny, Moscow region 141700, Russia, and [⊥]Intel Corporation, 2200 Mission College Boulevard, Santa Clara, California 95054-1549, United States. [||]Deceased.

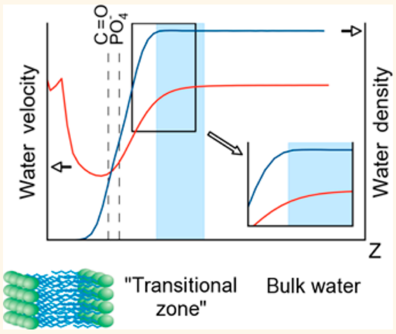

ABSTRACT The atomic-scale diffusion of water in the presence of several lipid bilayers mimicking biomembranes is characterized *via* unconstrained molecular dynamics (MD) simulations. Although the overall water dynamics corresponds well to literature data, namely, the efficient braking near polar head groups of lipids, a number of interesting and biologically relevant details observed in this work have not been sufficiently discussed so far; for instance, the fact that waters "sense" the membrane unexpectedly early, before water density begins to decrease. In this "transitional zone" the velocity distributions of water and their H-bonding patterns deviate from those in the bulk solution. The boundaries of this zone are well preserved even despite the local (<1 nm size) perturbation of the lipid bilayer, thus indicating a decoupling of the surface and bulk dynamics of water. This is in excellent agreement with recent experimental data. Near the membrane surface, water movement becomes anisotropic, that is, solvent molecules preferentially move outward the bilayer. Deep in the membrane interior, the velocities can even exceed those in the bulk solvent and undergo large-scale fluctuations. The analysis of MD trajectories of individual waters in the middle part of the acyl chain region of lipids reveals a number of interesting rare phenomena, such as the fast (*ca.* 50 ps) breakthrough across the membrane or long-time (up to 750 ps) "roaming" between lipid leaflets. The analysis of these events was accomplished to delineate the mechanisms of spontaneous water permeation inside the hydrophobic membrane core. It was shown that such nontrivial dynamics of water in an "alien" environment is driven by the dynamic heterogeneities of the local bilayer structure and the formation of transient atomic-scale "defects" in it. The picture observed in lipid bilayers is drastically different from that in a primitive membrane mimic, a hydrated cyclohexane slab. The possible biological impact of such phenomena in equilibrated lipid bilayers is discussed.

KEYWORDS: computer simulations · membrane permeability for water · model lipid membrane · spontaneous transmembrane water transfer · water–lipid interactions · water diffusion · water H-bonding

It is commonly accepted now that the concept of the membrane as a two-dimensional homogeneous mixture of lipids, proteins, and other components should be reconsidered based on modern experimental and computational data (see refs 1 and 2 for reviews). According to the latest data, cell membranes are rather heterogeneous in their physicochemical properties, containing a wide variety of domains differing in size, composition, lifetime, and so on.[2−5] In addition, these systems are highly dynamic and can reveal large-scale fluctuations even in equilibrium. It is noteworthy that the above phenomena occur not only in such multicomponent systems as cell membranes, but also in rather simple model membranes, one- and two-component lipid bilayers.[6,7] The complex character of cell membranes seems to be a fundamental intrinsic property that plays a vital role in their biological functioning, namely, the response to external signals (*e.g.*, the insertion of membrane peptides, proteins and other molecules; changes of temperature, pH, ionic strength; mechanistic exposure, and so on).[2,4,8]

Water is one of the crucial constituents of lipid membranes; it determines their self-assembly, interactions with other cellular

* Address correspondence to efremov@nmr.ru.

Received for review August 13, 2013 and accepted September 26, 2013.

10.1021/nn4042392

components, and fine-tuned adaptation to a large number of biological processes during the cell life.[9,10] Water molecules involved in the building and maintenance of cell membranes exhibit very different properties depending on their location with respect to the lipid bilayer and, therefore, on their interactions with neighboring molecules.[8,11] Thus, water's translational diffusivity in membranes drastically changes across the depth of the lipid bilayers. Being similar to bulk water at distances above ~4 nm, it decreases 2−3- and 6−7-fold in the vicinity of lipid headgroups and on the boundary of the acyl chain region, respectively.[12] Several types of water are usually considered: bulk water; near-interfacial water, water strongly bound in the polar headgroup region of lipids, and very few water molecules penetrating deep into the hydrophobic acyl chain region of the membrane.[13−16] Such a classification is often made based on the degree of mobility of water, which is measured by NMR, ESR, and IR methods, electrical conductivity measurements, and incoherent neutron scattering[11,15,17,18] or calculated *via* molecular dynamics (MD) simulations.[11,13,16,19,20]

It was shown that in the interfacial zone, water density does not monotonically decrease toward the bilayer center. Instead, the existence of at least two molecular-scale intrinsic hydration layers was detected in experiments[21] and computer simulations.[16] Finally, in several computational studies it was shown that water mobility even increases in the bilayer center.[13,22] Recently, quite a similar conclusion was made in experimental work.[12] In particular, it was found that highly dynamic hydration water in the lipid interior does not necessarily correlate with a high water content within the lipid bilayer. Such a complex behavior of water molecules is explained by their ability to participate in strong H-bonding interactions with carbonyls and phosphates of lipid headgroups. This, in turn, results in the formation of dynamic clusters of lipids, water, and ions.[7,8,25,26] Therefore, despite the fact that a knowledge of these parameters is necessary to understand on the molecular level the structural and dynamic behavior of hydrated lipid bilayers, the molecular basis of water diffusivity in membranes is still a subject of debate.

The issue was considered in a number of experimental and computational studies, and some recent reviews address this topic.[8,27] As a result, it was established that the detailed characteristics of both lateral and transversal diffusion of water seriously depend on lipid composition, hydration degree, temperature, and other features of the studied water−lipid system.[22,28] For instance, the polyunsaturation of lipids leads to increased water permeability and lower activation energy for water permeation due to looser lipid packing.[29] On the other hand, it was shown experimentally that water permeability correlates most strongly with the area per lipid and is poorly correlated with bilayer thickness and some other structural and mechanical properties of a number of phosphatidylcholine (PC)-based bilayers.[30] Hence, the dependence of water dynamics on the lipid bilayer composition is not straightforward, thus calling for further analysis.

One of the most intriguing observations made for biomembranes is the occurrence of water molecules deep in the hydrophobic bilayer core.[31,32] According to different estimations made for PC-containing lipid bilayers,[13,22,33] the free energy barrier for water transfer from bulk solvent to the membrane center is about 4−7 kcal/mol, thus making water concentration inside the bilayer very low—it corresponds to a partition coefficient of about 10^{-5}, similar to water/g-hexadecane systems.[34] Despite this, such events were well registered in experiments[18] and computer simulations.[8,32,35] So far, a coherent picture based on the literature data is that there is a very small number of water molecules within the hydrophobic bilayer region that rapidly translate through the bilayer with local diffusivities in the order of $(0.3-0.5) \times 10^{-9}$ m^2/s, as part of water clusters or transient pores.[12] This raises the question about the detailed molecular mechanism of spontaneous water permeation inside a very hydrophobic (and therefore "alien" for water) environment. An understanding of such phenomena is indispensable for the elaboration of adequate physical models of cell membranes, which can explain and rationalize a large set of recent data on the complex structural and dynamic behavior of even the simplest (one- and two-component) lipid bilayers. Among them are clustering/domain formation, the appearance of defects and pores, transport and diffusion properties, and so on.

There exist different models explaining the mechanisms of passive deep water penetration inside lipid bilayers. One of the earliest views is the solubility diffusion, which is based on the assumption that water is homogeneously distributed in the membrane.[12,29,31] Later, this model was modified[15,30] to take into account the strong dependence of such effects on the area per lipid values, in contrast to the role of the bilayer thickness. However, because of their continuum character, these approaches were unable to delineate the fine microscopic details of water−membrane interactions. This stimulated the development of different atomistic models. One of such hypotheses is that water permeates and diffuses across the lipid bilayer, not as lipid-solubilized molecules, but in small transient (hydrophobic) pores,[12,28] the so-called "transient pore model". According to it, such "trapped" waters continue to display high local diffusion coefficients whose values are relatively unaffected by direct, local, lipid environments (*e.g.*, lipid density, *etc.*). Finally, an original mechanism of water permeation into PC bilayers has been proposed recently by Pandey *et al.*[36] In this computational model, large-scale movements of trimethyl ammonium groups of PC act as a water carrier, thus pumping water molecules into the interfacial region of the bilayer.

Hence, as can be seen, the factors driving spontaneous water penetration into the nonpolar core of the lipid membrane are still a subject of active discussion. Therefore, data which may shed a new light on the problem are well-timed. Computer simulation techniques are believed to be especially helpful in this case because they are capable of providing atomistic details of water movements in a highly heterogeneous and dynamic membrane environment. It is important to note that in most of the simulation studies reported so far (see above), water molecules were artificially (often, "manually") implanted into the central part of pre-equilibrated lipid bilayers. Then, constrained or unconstrained molecular dynamics (MD) simulations were carried out to assess the behavior of these waters starting from such non-natural configurations.[13,22,33,37,38] These approximations were employed to obtain adequate statistics; the spontaneous penetration of water into the acyl chain region of lipid bilayers is a rare event which demands long-term MD analysis of large water–lipid systems. At the same time, the application of external driving forces (*e.g.*, constraints) can distort water behavior in the membrane. We therefore suggest that the problem of passive water diffusion in lipid bilayers can benefit from further systematic study on an atomic level.

The crucial questions here are the following: (1) Do molecules penetrate into the hydrophobic interior of lipid membranes without any artificial constraints and external driving forces? (2) If so, are these individual waters or water clusters? (3) What are the driving forces for these phenomena? (4) Does the dynamics of water in lipid bilayers differ from that in an artificial nonpolar organic slab?(5) To what extent are water properties sensitive to local perturbations of the membrane? (6) How adequate are the simulation results? Are they tied to experiments? To inspect such events with high time and spatial resolution, we have in this work carried out large-scale unconstrained MD simulations of a series of hydrated one- (dioleoylphosphatidylcholine (DOPC), dipalmitoylphosphatidylcholine (DPPC), dioleoylphosphatidylserine (DOPS)) and two- (DOPC/DPPC 9:1; palmitoyl-oleoylphosphatidylglycerol (POPG)/palmitoyloleoyl-phosphatidylethanolamine (POPE) 3:1 mixture with embedded lipid-II molecule) component lipid bilayers as well as a water/cyclohexane slab. A special emphasis was placed on the analysis of the MD trajectories of individual water molecules occasionally entering into the lipid bilayer core. The atomic-scale picture of water movement and interactions with neighboring molecules reveal several unexpected features, which may have a serious biological impact and extend our understanding of the complex structural/dynamic properties of model cell membranes.

RESULTS AND DISCUSSION

The study is organized as follows. First, a detailed analysis of water dynamics in the DOPC bilayer was carried out. The main attention here was given to changes of water properties along the membrane normal (axis *Z*). The following parameters of water were considered: velocity (modulus, orientation), local diffusion coefficient, free energy of water/bilayer transfer, and H-bonding patterns. (We should note that the velocities of individual water molecules were calculated based on local diffusivity data obtained for consecutive MD snapshots (see Materials and Methods). Therefore, they do not correspond to momentary velocities. This topic is discussed in more detail elsewhere.[22]) To inspect whether the dynamic behavior of water inside a hydrated lipid bilayer is sensitive to chemical composition of the latter, MD simulations were also performed for a set of membranes with physicochemical properties rather different from those of the DOPC: DPPC, DOPC/DPPC (9:1), DOPS, and POPG/POPE (3:1). In addition, the same computational protocol was applied to one nonlipid membrane, a cyclohexane slab in water. The first system, the DPPC, has a similar zwitterionic polar head, but saturated fatty chains. The second one was chosen to assess the effect of mixing relatively rigid (DPPC) and fluid (DOPC) lipids. The POPG/POPE bilayer was also simulated with a biologically important additive, a lipid-II molecule. (Lipid-II is a crucial and highly specific target of antibiotic action.[23]) These two systems (with and without lipid-II) were specially taken to check to what extent strong local perturbations of the lipid bilayer induced by the lipid-II may affect water dynamics. Note that the PC-based bilayers imitate well the membranes of eukaryotic cells. In contrast, the DOPS and especially the POPG/POPE bilayers represent a model of a membrane formed by anionic lipids, which are specific for bacteria. Finally, a cyclohexane slab was used to compare the role of native lipids in determining water properties with those observed in an artificial hydrophobic layer separating two reservoirs of water. To get an insight into the molecular mechanisms of water behavior in the model membranes, the MD trajectories of individual waters spontaneously penetrating deep into the hydrophobic core of all the studied systems were analyzed. On the basis of these statistics, atomic-scale mechanisms determining permeability for water of different model membranes were delineated.

The Transversal Dependence of Water Velocity in a Hydrated DOPC Bilayer. The dependence of the average absolute velocity values on the coordinate z ($v_w(z)$) is shown in Figure 1. For comparison, the value v_w obtained for pure water is also indicated with a horizontal arrow on the left *Y*-axis. As it was reasonable to expect, the plots are symmetrical with respect to the membrane central plane; this is caused by the equivalent composition of the monolayers and water on the two sides. It can be seen that far from the lipid bilayer core, at distances >3.7 nm, the mobility of water is similar to that in an aqueous solution (*ca.* 57 m/s). (Hereinafter, the values

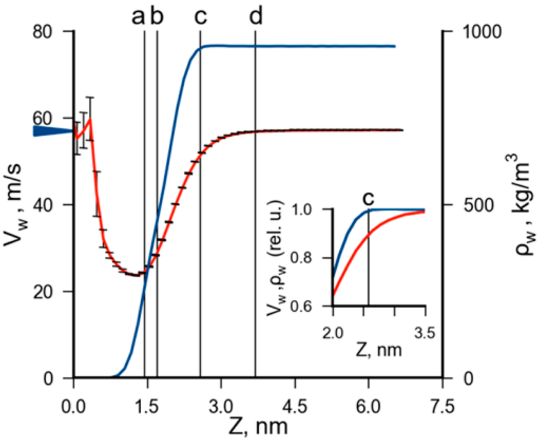

Figure 1. The average absolute velocity (v_w, red line) and density (ρ_w, blue line) of water in the DOPC bilayer plotted as a function of the distance from the bilayer center (*z*). The middle of the bilayer corresponds to $z = 0.0$ nm. The positions of the density peaks for carbonyl and phosphate groups of the DOPC are shown with vertical lines marked "a" and "b", respectively. The boundaries of the "transitional zone" for water (see text) are indicated with vertical lines marked "c" and "d". The horizontal arrow shows the average value of v_w in a free water box. (Inset) Augmented view of the "transitional zone" closest to the bulk water region. Here, water velocity and density are given in relative values, thus allowing comparison of the curve shapes. An averaging was done over an ensemble of water molecules in each frame and over the MD trajectory (see Materials and Methods). The statistical errors for the velocity plot are denoted with vertical bars. For the density plot they are much smaller and therefore are not shown.

of *z* are counted from the bilayer center, and in the case of the cyclohexane slab, from its middle plane.) Upon approaching the membrane, water molecules reduce their velocity by up to 2.5 times. The velocity curve reveals a prominent minimum near $|z| = 1.27$ nm. As follows from the analysis of density plots for various components of the DOPC bilayer (Figure S1 in the Supporting Information), this region corresponds to the location of strong water binders, phosphates, carbonyls, and trimethyl ammonium groups. Here, water molecules form H-bonds with polar lipids heads, thus slowing down and losing their kinetic energy. It is noteworthy that similar minima of $v_w(z)$ are also observed using much more limited statistics — for an arbitrary water molecule monitored on the whole MD trajectory and for an ensemble of waters taken from two arbitrary consecutive MD-frames (Figure S2).

The intriguing feature of the $v_w(z)$ plot is the strong velocity growth upon the water's penetration inside the membrane, at $|z| < 1.27$ nm. Thus, in the bilayer center, the velocity of waters can be as high as in the bulk solvent. It can also be seen that the values $v_w(z)$ reveal serious fluctuations. Despite the fact that the events when water molecules are found in the extremely hydrophobic core of the membrane are rare, 100-ns long MD trajectories allow for the accumulation of reasonably good statistics. Of course, the fine details of the velocity plot in the membrane center can change, but the overall picture does not. This supports the conclusions made above. Interestingly, when moving toward the membrane interior, v_w starts to decline significantly earlier than water density starts to drop meaningfully (by 0.1% at $|z| < 2.58$ nm). Also, according to the lipid density distributions along the membrane normal (Figure S1), no bilayer components are found in this region. In other words, such a peculiar "braking" of waters occurs already in an environment where each water molecule still has the same number of neighbors and reveals unperturbed radial distribution functions, such as in an aqueous solution. One can assume that the appearance of the "transitional zone" is related to the distribution of dipole potential along the bilayer normal. But this is not the case; detailed analysis shows that the electrostatic characteristics of the water/lipid interfaces reach a plateau already at $|z| < 2.5$ nm.[8,24] More details about the structural and dynamic properties of water in this "transitional zone" (between the bulk and interfacial water, at $2.58 < |z| < 3.70$ nm) are given in the next section. As seen in Figure S3, the overall trend in the plot $v_w(z)$ obtained for the DOPC, prominent minima in the headgroup regions and several maxima in the hydrophobic membrane core, is well preserved for all the lipid bilayers under study. On the other hand, the details can vary. The most striking difference is observed between the DOPS membrane and the others. This is reflected in larger distances between the minima obtained for opposite lipid monolayers (Δz) and their smaller depth. It can be seen that the values of Δz for the DOPC, DPPC, and DOPS bilayers (2.54, 2.84, and 3.40 nm) correlate with the bilayer thickness, measured in experiments as the distance between the phosphate density peaks of the monolayers (3.61, 3.81, and 3.90 nm).[38,39] Furthermore, it is interesting to note that the velocity plot for the DOPC/DPPC (9:1) system is much closer to that for the DPPC than the DOPC, although this bilayer contains only 10% of DPPC lipids. This fits well with our earlier observation concerning large changes of integral structural/dynamic parameters of the DOPC membrane upon the addition of even a small amount of the more rigid DPPC to it.[7] On the basis of the dynamic behavior of water in lipid bilayers of different composition and therefore, different physicochemical properties, we can conclude that the picture of transversal distribution of water velocities can be quite specific for a particular bilayer. Thus, the above-mentioned peculiarities of velocity distribution in the DOPS bilayer can be related to the sharp mosaic nature of its surface,[26,41,42] which exhibits prominent hydrophilic and hydrophobic clusters. The latter is not true for PC-containing zwitterionic membranes, where the water/lipid boundary is rather smooth and does not reveal such "blazing spots" of hydrophobicity.[42] On the other hand, the comparison of average order parameters of acyl chains in the DOPS and DOPC bilayers indicates

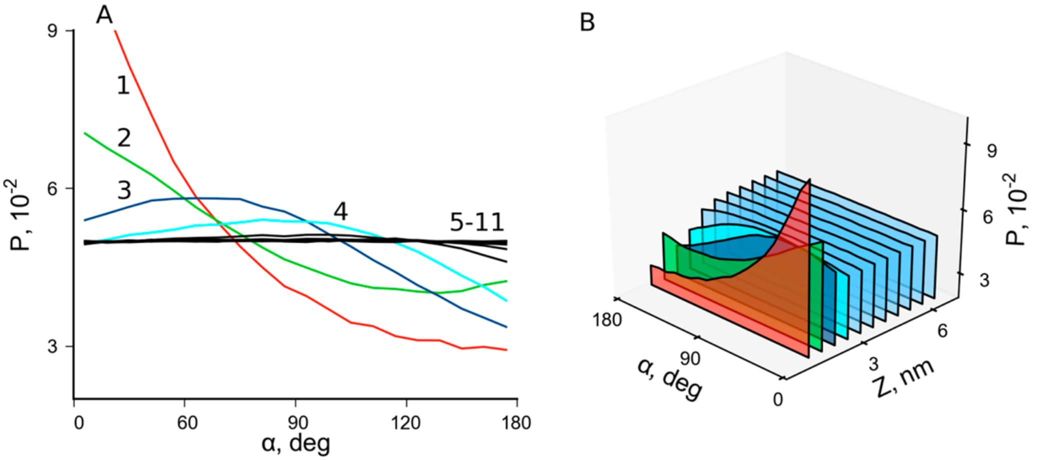

Figure 2. The anisotropy of water moves in the DOPC bilayer. (A) The averaged distributions of water molecules over the orientations of their velocity vectors with respect to the membrane normal (α) at different depth (*z*). Here, α is the angle between the velocity vector and the bilayer normal, *z* is the distance from the bilayer center. *P* is the relative number of waters with a given value of α (normalized over the total number of water molecules). Curves 1–11 correspond to values of *z* of 1.07, 1.60, 2.14, 2.67, 3.21, 3.74, 4.28, 4.81, 5.35, 5.88, and 6.42 nm, respectively. It is seen that deep in the membrane core (curves 1, 2) waters move outward the bilayer, whereas at $|z| > 3.2$ nm (curves 5–11), water movements are isotropic. (B) The same distributions as in panel A, but shown in 3D as viewed from the bilayer center ($z = 0$ nm).

that the former is more rigid. Hence, we should note that despite some correlations observed, the casual relationships between water dynamics and integral bilayer properties remain elusive on a molecular level and require further studies.

Besides the average absolute velocities, additional information about water dynamics is provided by the orientations of water velocity vectors with respect to the membrane normal (angle α) at different *z*. This is discussed in the next section.

The Anisotropy of Water Movements near and inside the DOPC Bilayer. The corresponding distributions over the values of α are shown in Figures 2. As it was reasonable to expect, far from the bilayer center water molecules move isotropically, in all directions. In contrast, starting from *ca.* 2.85 nm from the middle of the DOPC bilayer, a prominent anisotropy in the orientation of water movements appears. This is reflected in the gradual reduction of the number of waters moving toward the membrane (α > 90°) and growing the distribution curve at lower values of α. Thus, in the water–lipid interfacial region, at $|z|$ between 2.3 and 2.7 nm, they move almost parallel to the membrane plane (α-distribution has maximum at 80–100°). Deeper into the membrane (at $|z| < 1.8$ nm, in the region of phosphate and carbonyl groups of DOPC), the maximum of the angular distribution shifts to 0–30°, indicating that most of the waters move backward along the membrane normal. In other words, water molecules are escaping the membrane core. The effect is especially sharp deep inside the bilayer, at $|z| \approx$ 0.7–0.8 nm. At smaller $|z|$ (below the C═C bond of the DOPC and between the lipid leaflets), the distribution curves become too noisy, due to poor statistics for waters found in the membrane's central part. Such individual spikes occur at different angle values, thus demonstrating multidirectional movements of single water molecules deep inside the hydrophobic zone.

Besides angular distributions, the movements of water molecules at different z were also characterized in terms of two-dimensional distributions "average absolute velocity/average angle of velocity vector with the bilayer normal". The corresponding plots (v_w, α) for various membrane depths are shown in Figure S4. It can be seen that at each angle value the velocity distributions have a Maxwell-like form. At the same time, depending on the *z*-coordinate, their parameters (peak height, position and bandwidth) can significantly change at different values of α. Thus, in the bulk water, all the distributions are similar because there is no anisotropy in water movements. When approaching the membrane center, the aforementioned augmentation of the integral intensity at large α values is accompanied by an increase of the most probable velocity. Therefore, in the central membrane parts, the fraction of molecules moving toward the membrane exteriors (α < 90°) and their absolute velocities become bigger. This creates a kind of flow out of the membrane's middle plane determined by the gradients of water concentration and the free energy of water/membrane transfer (see Figure 3), which are directed outward and toward the membrane center, respectively.

In summary, the presence of the lipid bilayer breaks the isotropy of water movements in the region where the first lipid groups appear. Interestingly, such an anisotropy has a different preferential direction depending on the membrane depth.

Taking into account the quite unusual properties of water velocities in the lipid bilayer center,—to the authors' knowledge, at least some of these results have

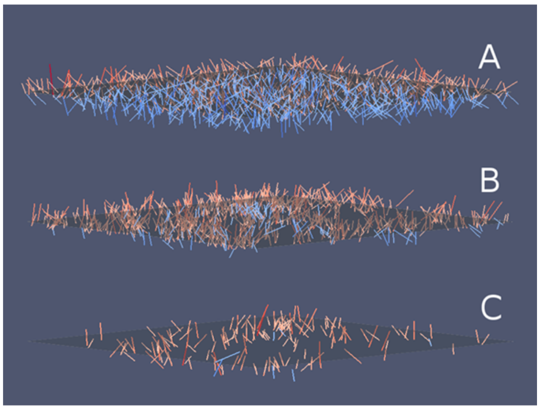

Figure 3. The distributions of average water velocity vectors at different distances from the DOPC bilayer center (z): (A) $Z \in [3.0\ \text{nm}, 3.2\ \text{nm}]$, $\Delta t = 30$ ps; (B) $Z \in [1.2\ \text{nm}, 1.4\ \text{nm}]$, $\Delta t = 500$ ps; (C) $Z \in [0.5\ \text{nm}, 0.7\ \text{nm}]$, $\Delta t = 20$ ns. Only vectors with a z-component of the velocity vector above 24 m/s are shown. Vectors directed toward and outward of the membrane center are indicated with blue and orange colors, respectively.

not been reported yet—we also calculated more convenient characteristics of water dynamics, such as local diffusion coefficients (D_w) along the membrane normal.

Local Diffusion of Water along the Membrane Normal. These parameters were previously reported by several groups based on experimental[32,43] and computational[13,22] studies of different PC-containing lipid bilayers. The plot $D_w(z)$ obtained here for the DOPC bilayer is shown in Figure 4. It can be seen that in the bulk solvent (at $|z| > 3.7$ nm), D_w is constant (*ca.* 6×10^{-5} cm^2/s) and coincides well with the values known for pure water.[22]

Upon further movement toward the bilayer center, D_w reveals "S-shaped" damping and reaches its minimal values (min D_w) equal to 0.3×10^{-5} cm^2/s on the interval $0.7 < |z| < 1.5$ nm. Therefore, the slowest transversal diffusion is observed in the region between $C{=}O$ and $C{=}C$ groups of lipids, where the density of water is approaching zero. In contrast, in the middle part of the membrane, the diffusion is very fast and reveals strong fluctuations. Here, the values of D_w can reach 12×10^{-5} cm^2/s exceeding those in the bulk solvent. Therefore, the amplitude of the effect of diffusion growing (the difference between its minimal and maximal values (ΔD_w)) is *ca.* 12×10^{-5} cm^2/s. The overall picture is quite similar for all lipid bilayers under study (see Figure S5), although the exact parameters of the curves (the beginning of the fluctuation region, positions of minima, *etc.*) may vary.

The comparison of the resulting D_w-plots obtained for the DPPC bilayer with those reported by other authors[13,22] shows a rather good agreement in the region of $|z| > 0.7$ nm. This proves the overall correctness of the computational protocol applied in this work. At the same time, there are certain discrepancies between the three studies. One is the amplitude of D_w growing in the thin (1.4 nm width) central layer of the membrane (ΔD_w, see above), where fast water movements and strong fluctuations are observed. In our work, the values of ΔD_w and min D_w are about 1.1×10^{-4} and 0.2×10^{-5} cm^2/s. An increase of water diffusion was earlier observed in works,[13,22] although in the latter case the effect in the DPPC was smaller; the values of ΔD_w and min D_w were *ca.* 0.3×10^{-4} and 0.1×10^{-4} cm^2/s, respectively. The results of the present paper are in much better agreement with the work,[13] where the corresponding values were 1.4×10^{-4} and 0.1×10^{-5} cm^2/s, respectively; *i.e.*, diffusion growing in the membrane center was very prominent. At the same time, one important difference still exists, namely, the shape of the minima on the D_w plots. In our work, this is a basin-like flat region protruding from 1.5 to 0.7 nm from the bilayer center (Figure S5), while in the paper,[13] the minimum located at $|z| \approx 1.4$ nm is rather sharp. We assume that the discrepancies are caused by the fact that in both cited publications MD simulations were performed with the water molecules being restrained in the bilayer center, whereas in the present study, only the spontaneous water penetration into the membrane was considered. We should also note that the increase of water diffusion inside the DOPC and DOPS bilayers was not observed in ref 16; the values of D_w were minimal in the bilayer center and monotonously grow toward the bulk water. Moreover, inside the headgroup regions (near $C{=}O$ groups) the translational motion of water molecules was slowed down compared to the bulk water by a factor of 100−500, which is much higher than in the three other studies discussed above. Finally, in some of the other recent studies,[12] the increased mobility of water inside the membrane was not detected either.

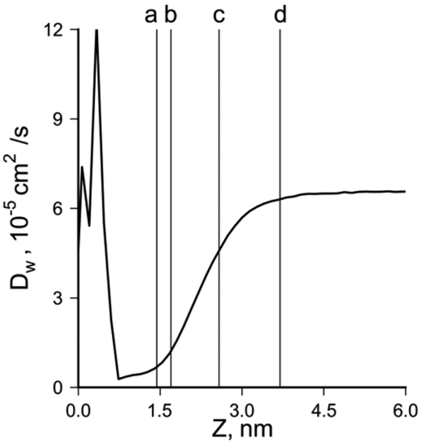

Figure 4. The average local diffusion coefficient D_w of water in the DOPC bilayer plotted as a function of the distance from the bilayer center (z). The middle of the bilayer corresponds to $z = 0.0$ nm. The positions of the density peaks for carbonyl and phosphate groups of the DOPC are shown with vertical lines marked "a" and "b", respectively. The boundaries of the "transitional zone" for water (see text) are indicated with vertical lines marked "c" and "d". Oher details are the same as in the legend to Figure 1.

Apart from local diffusion, we also compared the calculated free energy barriers for water transfer across the lipid bilayers under study with those reported earlier by other authors.

Free Energy Profile. The free energy profiles along axis *Z*, d$G(z)$, are plotted in Figure S6. It can be seen that there is a high (~7 kcal/mol) energy barrier for the water transfer across the DOPC bilayer. In accordance with the way of d$G(z)$ calculation, based on water density data (see Materials and Methods), the energy begins to grow at $|z| \approx 2.5$ nm, synchronously with the water density drop, but with a delay regarding the $v_w(z)$ and $\alpha(z)$ plots. At the bilayer center, the results are quite noisy due to the growing statistical error of MD data processing caused by the limited amount of information. Obviously, the prominent energy gradient directed toward the membrane center creates a force acting on water molecules in the opposite direction, thus explaining their collective movement out of the hydrophobic lipid core (see above). Similar plots for other lipid bilayers under study are also given in Figure S6. It can be seen that all of them have close values of barrier height, but differ slightly in width. As expected, the largest width is observed for the thickest membrane, the DOPS. Interestingly, despite the prominent transversal heterogeneity of structural and dynamic properties of hydrated lipid bilayers (including the water velocities distributions considered above), the water density and the free energy profiles exhibit quite a monotonous character without local extremes in the regions containing lipid groups forming strong H-bonds with waters (see *e.g.*, Figure 1).

The free energy profiles for all lipid bilayers under study match the data reported by other groups well.[13,22] At the same time, one should note that these d$G(z)$ plots were obtained using nonpolarizable force fields. Recent MD simulations with polarizable charge equilibration force fields[33] demonstrated a reduced free energy barrier of ~5 kcal/mol for the transfer of a water molecule from the bulk to the lipid interior. This does not change the above-mentioned overall conclusions reached in this work.

The dynamics of water in the presence of a lipid membrane strongly depends on the characteristics of hydrogen bonds (H-bonds) formed with neighboring water and lipid molecules. These results are described below.

Water H-Bonding in the Membrane. Figure 5A shows the average number of water−water (n_{ww}) and water−lipid (n_{wl}) H-bonds per water molecule at different values of *z* in the DOPC bilayer. Similar data obtained for other lipid−water systems are plotted in Figure S7A. It can be seen that in the case of the DOPC, n_{ww} monotonously drops on the interval of $|z|$ from 2.56 to 0.55 nm, whereas n_{wl} in this region displays a bell-shaped curve with a maximum at $|z| = 1.27$ nm. The latter one is not far from the locations of strong water binders, carbonyl and phosphate groups of PC lipids (vertical lines marked "a" and "b", respectively). Overall, the total number of water H-bonds ($n_{w\text{-total}} = n_{ww} + n_{wl}$) follows the water density profile ($\rho_w(z)$) along the membrane normal. At the same time, a detailed inspection of these plots (data not shown) demonstrates that the shapes of the two curves are not identical. When moving toward the membrane center, the deviation of $n_{w\text{-total}}$ from the values observed in the bulk solution begins already at $|z| \approx 2.75$ nm, earlier than water density changes appear. This can explain the origin of the aforementioned "transitional zone" (see above), where the velocities of waters but not $\rho_w(z)$ deviate from their bulk values. Analogous curves obtained for the other three bilayers reveal quite similar general features. The differences are related to exact parameters like the distance where the curve reaches zero, and so on. Such deviations are especially prominent for the DOPS system. First, here the H-bonds disappear at $|z| = 0.76$ nm, thus making the hydrophobic zone without hydrogen bonds much thicker. Second, for the DOPS bilayer, the *z*-dependence of the average number of water−water H-bonds per water molecule reveals a shoulder at $|z| \approx 1.5$ nm, which corresponds to the C=O groups of lipids. Finally, there are no H-bonds in the middle part of the DOPS membrane (this is also discussed below).

Besides the number of water H-bonds, the analysis of their average lifetimes (τ_{Hbn}) is very important. As can be seen in Figure 5B, such values grow significantly when moving from the bulk water toward the membrane center, from 12 ps to *ca.* 50 ps in the DOPC bilayer. This is certainly related to the replacement of inter-water bonds by the stronger water−lipid ones. Plot $\tau_{Hbn}(z)$ reveals a broad maximum centered at $|z| \approx 0.98$ nm and then rapidly dropping to reach zero at $|z| = 0.35$ nm. As noted by M. Berkowitz *et al.*,[16,27] the smaller amount of H-bonds in the lipid bilayer tends to be compensated by an increase in their stability expressed in terms of τ_{Hbn}. Unlike n_{Hbn}, the values of τ_{Hbn} remain almost unchanged at a constant density of water (data not shown), and therefore, the stability of inter-water H-bonds is not affected in the "transitional zone" (see above). Interestingly, the average lifetime of H-bonds formed by waters in model membranes and its dependence on *z* are sensitive to the bilayer composition. Thus, the maximum values of τ_{Hbn} increase in the row: DOPS (20 ps) < DOPC (50 ps) < DPPC (57 ps) < DOPC/DPPC (9:1) (68 ps) and the difference can exceed 3.4 times. It is noteworthy that positions of the maxima for PC-based lipids are shifted toward the membrane center, relatively far from the peak densities of phosphates and carbonyls of head groups (the latter ones are depicted in Figure 5B and Figure S7B with vertical lines). On the contrary, in the anionic DOPS bilayer, the $\tau_{Hbn}(z)$ plot exhibits the most prominent peak much closer to these lipid groups ($|z| \approx 1.64$ nm) (Figure S7B).

Water Dynamics in a Non-Natural Membrane: A Hydrocarbon Slab in an Aqueous Solution. As discussed above, despite the chemical composition, all four lipid bilayers considered in this study exhibit quite a similar atomic-scale picture of

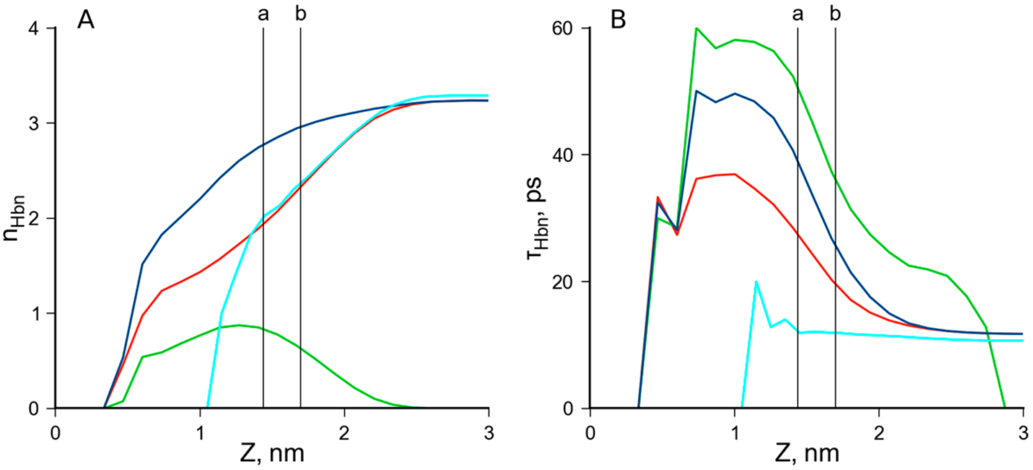

Figure 5. The average H-bonding parameters per water molecule in the DOPC bilayer and in a cyclohexane slab plotted as a function of the distance from the bilayer (or slab) center (*z*). (A) The number (n_{Hbn}) of water−water (red), water−lipid (green), and all types (blue) of H-bonds in the DOPC, along with the number of water−water H-bonds in a cyclohexane slab (cyan). The positions of the density peaks for carbonyl and phosphate groups of the DOPC are shown with vertical lines marked "a" and "b", respectively. (B) The lifetime (τ_{Hbn}) of H-bonds in the DOPC bilayer and cyclohexane slab. Colors are similar to those in panels A. Other details are the same as in the legend to Figure 1.

water behavior near the membrane surface and inside the hydrophobic core. The observed minor differences are caused by peculiarities of the structural/dynamic organization of the bilayers and are mainly related to the quantitative parameters of the calculated velocity distributions, diffusion coefficients, and free energy profiles. Is this tendency correct for other apolar media separating two volumes filled with water? To gain insight into this problem, we carried out MD simulations of a hydrophobic slab composed of cyclohexane molecules and hydrated with water from both sides. The thickness of the slab (4.08 nm) was taken quite close to that of the lipid bilayers under study. Being rather simpler for computer simulations, this system in certain important aspects (the thickness of the hydrophobic layer, resistance to water penetration, and so on) resembles cell lipid membranes. This is why cyclohexane and other apolar organic molecules are widely used as membrane mimics in modeling peptides and proteins.

The results of water dynamics in such a system are shown in Figure 5 (characteristics of H-bonds), Figure 6 (average absolute velocity along the slab normal), Figure S5 (average local diffusion coefficient), Figure S6 (free energy profile across the slab), and Figure S8 (anisotropy of water movements along the slab normal). It can clearly be seen that, overall, the diffusivity of water near the hydrocarbon "membrane" surface resembles that in the lipid bilayers described above, although a number of remarkable differences exist as well. They are the following: (1) The absolute velocity minima, which are deep (∼30 m/s) in lipid bilayers (Figure 1 and Figure S3), are almost negligible (<6 m/s) on the cyclohexane/water interface. This indicates that the effect of water braking here is very modest because no H-bonding partners exist for water. As a result, strong fluctuations of water movements occur almost over the whole thickness of the slab. (2) The "transitional zone" near lipid bilayers is much wider (0.96 nm for the DOPC) than in the vicinity of the cyclohexane slab (0.57 nm at $|z|$ between 2.48 and 3.05 nm). (3) When traveling from outside toward the slab center, the anisotropy in the angular distribution of water velocities begins later than in lipid bilayers, when ρ_w is already much smaller than in the bulk solvent. (4) Near the lipid interface, ρ_w deviates from its bulk values when the first lipid groups already occur in the solution, whereas this is not the case for the slab; here, water and cyclohexane densities change in a strictly opposite manner, starting from $|z| = 2.48$ nm. Furthermore, water density in the slab reaches zero much faster (on the interval 1.25 nm) than in the DOPC (2.03 nm). Therefore, the slab/water boundary is much more narrow than the water−bilayer interface, and the waterless region is thicker in cyclohexane as compared with the DOPC, 2.46 *vs* 1.10 nm, respectively. (5) The parameters of the water−water H-bonds near and inside the slab are drastically different from those in the bilayers. This is especially prominent for the lifetimes (τ_{Hbn}) of such bonds (Figure 5B). In cyclohexane, plot $\tau_{Hbn}(z)$ reveals only a moderate (increasing by ∼30%) maximum at $|z| = 1.25$ nm, where water density reaches zero. In contrast, in the DOPC bilayer, plot $\tau_{Hbn}(z)$ demonstrates a much higher peak (up to 300%), which is also shifted toward the membrane center (see above). (6) The free energy barrier in cyclohexane is ≈ 1 kcal/mol higher than those in lipid bilayers (Figure S6).

Hence, as it was reasonable to expect, a lipid bilayer, which is more complex in transversal distribution of physicochemical properties, exhibits more sophisticated dynamics of water on the interface and inside. The possible biological consequences of this are discussed later.

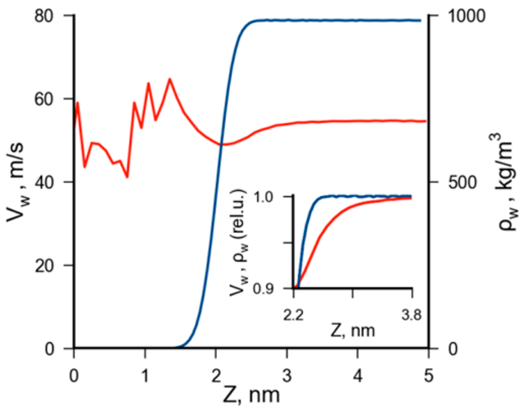

Figure 6. The average absolute velocity (v_w, red line) and density (ρ_w, blue line) of water in a cyclohexane slab plotted as a function of the distance from the bilayer center (z). The middle of the bilayer corresponds to z = 0.0 nm. (Inset) Augmented view of the "transitional zone" closest to the bulk water region. Here, water velocity and density are given in relative values, thus allowing comparison of the curve shapes. Other details are the same as in the legend to Figure 1.

As follows from the calculated average velocity distributions, very few water molecules observed in the lipid bilayer core and cyclohexane slab can exhibit unexpectedly high velocities and a specific "directional" character of movement. A detailed analysis of their behavior is required to understand the exact molecular mechanisms of such effects. This is considered below.

The Spontaneous Penetration of Water inside the Hydrophobic Membrane Core. Individual water molecules found in the membrane core, with $|z| \leq 0.7$ nm or $|z| \leq 0.5$ nm, were further considered as "events" (see Materials and Methods), and the "history" of such waters (hereinafter, any of them is denoted as water$_i$) was analyzed during the time interval when it was traveling from the bulk solvent into the membrane core and back to the bulk region. For each of the events, its temporal characteristics (start time and duration), along with plots $z(t)$, $v_w(t)$, and $D_w(t)$ were obtained. Furthermore, the following average parameters were calculated for each water$_i$ when it was present in the central zone of the membrane: (1) absolute velocity and its components; (2) z-coordinate; (3) total displacement and its components; (4) numbers of neighboring waters and H-bonds formed with them; (5) energy of van der Waals and electrostatic interactions of water$_i$ with its neighbors.

Such analysis reveals that two roughly distinct types of event, "fast" and "slow", can be delineated. Examples of the typical plots $z(t)$ and $E(t)$ for them are drawn in Figure 7. It can be seen that in both cases, water$_i$ is approaching the region of acyl chains ($|z| < 1.4$ nm) in a stepwise manner, but its subsequent behavior can be drastically different. In "fast" events, water$_i$ accelerates and leaves the nonpolar environment with a high speed, which can exceed that in the bulk solvent. As a result, water$_i$ either crosses the lipid bilayer or it is reflected from the membrane core and returns back to the polar zone on the same side. In both cases, the water molecule resides in the hydrophobic medium only *ca.* 50 ps (Figure 7A). In contrast, in "slow" events, water$_i$ is "roaming" for a relatively long time (up to 750 ps) in the middle part of the lipid bilayer (preferentially between the membrane leaflets, Figure 7B), and its velocity fluctuates in a wide range. One should also note that in events of both types, water$_i$ can be found on either side of the membrane because of the symmetry of the lipid bilayers used in the simulations.

An analysis of the intermolecular interactions of the considered water molecules with their neighbors reveals the following microscopic picture of the events:

•Upon transition from the bulk solvent to the region of polar headgroups of lipids, it gradually replaces part of its H-bonds with waters (from 3 to 4 to 0−1) by those with lipids (from 0 to 1−2). At this stage, the velocity of water$_i$ is decreasing, while the lifetimes of the H-bonds increase. This is reflected in the appearance of a minimum on the velocity plot (Figure 1) and a maximum on the $\tau_{\text{Hbn}}(z)$ plot (Figure 5B), respectively.

•Deep inside the membrane, in the hydrophobic acyl chain environment, water$_i$ loses all H-bonds with its neighbors. Here, it has no energetically favorable interactions with other molecules (except the rare cases when two H-bonded waters are simultaneously found there, see below). For instance, the electrostatic term in the potential energy function of water$_i$ reaches zero (Figure 7C,D) and the repulsive van der Waals contacts with hydrophobic chains of lipids are negligibly small. In such an "alien" environment, water$_i$ can develop a rather high speed and rapidly changes the direction of its movement. This continues for tens to hundreds picoseconds, until it reaches the regions with polar groups. Then, water$_i$ is slowing down due to H-bonding with lipid headgroups and interfacial water.

Inside the membrane, the lateral displacements of water$_i$ molecules strongly depend on the aforementioned types of events. In the case of "fast" events, the characteristic size of movements in *XY*-plane does not exceed 1 nm, while for the "slow" type, it is about 4−5 nm. In the latter case, the lateral diffusivity of water is much greater compared with the lipid head groups region, where only a small fraction of water molecules moves in the membrane plane.

It is interesting to compare the overall statistics of the events observed in the studied lipid bilayers and cyclohexane slab. The results for two central hydrophobic layers, with $|z| \leq 0.7$ nm (set "07") and $|z| \leq 0.5$ nm (set "05"), are given in Table S1. Several conclusions can be drawn based on these results:

1. The total number of events for sets 07 and 05 is drastically different for all systems except the DOPS; in the former case, they are much more frequent. Surprisingly, in the anionic bilayer (DOPS) the number of events in set 05 is almost the same as in other systems,

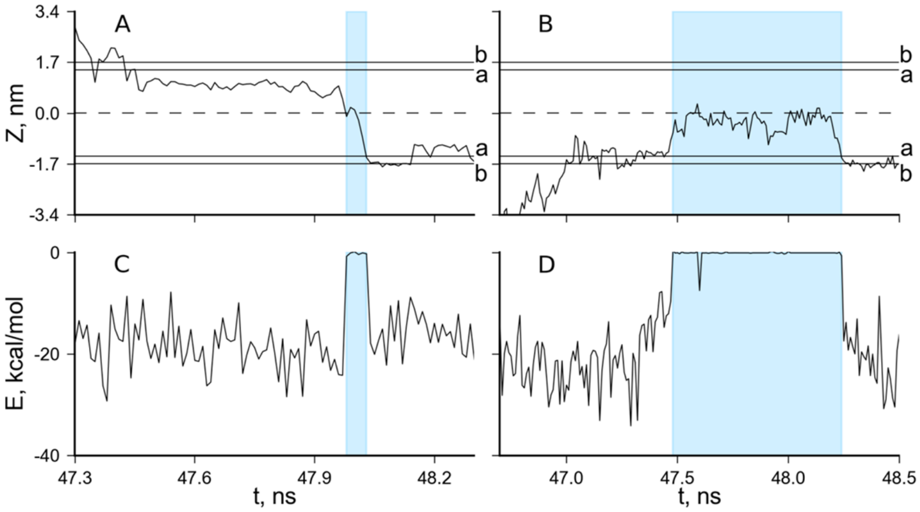

Figure 7. The history of a spontaneous water penetration into the DOPC bilayer. Fast (A and C) and slow (B and D) "events" of water traveling inside the hydrophobic core. (A and B) *z*-coordinate *vs* simulation time; (C and D) total energy of intermolecular interactions (electrostatic + van der Waals) of considered water molecules with their surroundings (*E*). The middle of the bilayer is marked with a dashed line. The positions of the density peaks for carbonyl and phosphate groups of the DOPC are shown with horizontal solid lines marked "a" and "b", respectively. The blue shading indicates regions where *E* is close to zero.

although it is much smaller than that in set 07. So, in the DOPS bilayer, almost all waters entering the hydrophobic core ($|z| < 0.7$ nm) are found in the central membrane zone ($|z| < 0.5$ nm), whereas in PC-bilayers most of the water molecules tend to be located near the upper boundaries of the core (data not shown).

2. The velocity distributions in the central part (set 05) and in its neighboring outer layers ($0.5 \text{ nm} < |z| < 07 \text{ nm}$) show that water molecules move much faster in the former case (data not shown). Moreover, in the membrane region with $|z|$ between 0.5 and 0.7 nm, water molecules move preferentially parallel to the membrane plane; the corresponding distributions over v_z reveal strong narrow peaks at $v_z = 0$ m/s, while at $|z| \leq 0.5$ nm, this picture is not yet so pronounced due to the appearance of waters moving along the membrane normal (data not shown). This fact is also reflected in the much smaller distances passed by water molecules in the membrane plane during the lifetime of the events from set 05.

3. The lateral distributions of the average coordinates (x,y) of the events have no visible peculiarities; the events are found in all regions on the bilayer plane (data not shown).

4. There are no prominent differences between the frequencies of the events from set 05 observed in all model membranes, including the cyclohexane. Also, the frequencies of water transitions between the monolayers are quite similar, about 1 event per 2.2−3.5 ns.

5. Although the vast majority of the events represent independent processes in time and in space, some exceptions occur. Thus, 2−4 simultaneous, but spatially distant, penetrations of waters into the membrane core (set 05) were detected in each system. Moreover, several of them (one—in the DOPC; two—in the DOPS; four—in the cyclohexane) revealed a "collective" character; in all the cases, two H-bonded water molecules were traveling in the extremely nonpolar environment on time scales of 30−170 ps. One example of such pair of events is shown in Figure S9.

A detailed tracing of all the found water$_i$ shows that their spontaneous entry into the central part of the membrane does not depend on any particular interactions with specific lipid groups as it was proposed in ref 36. Instead, the MD trajectory of a given water molecule is determined by randomly fluctuating structural and dynamic properties of its microenvironment, although some ill-defined correlations with the formation of membrane surface defects (like deep hollows, *etc.*) are observed. Further analysis of these effects is needed, but this is beyond the scope of this work.

Interestingly, the passive entry of waters into the core region of biomembranes was mostly detected for single molecules or (very rarely, see above) for pairs of them. No larger groups were observed. Although several sequential events of water passage were found, they were not accompanied by an assembling of waters deep in the lipid environment. This distinguishes our simulation results from some previous modeling data[22,37,44] considering H-bonded clusters of several waters forming transmembrane micro channels and/or defects. Here, we can just state that a spontaneous clustering of water inside the membrane was not observed in our work. On the other hand, the inspection of the radial distribution functions (RDFs) for water at different z shows that even in the low-density regions (at $|z| \approx 0.7-1.2$ nm) water molecules still form large enough clusters and have RDFs very similar to those in the bulk solvent (data not shown, see also ref 13). Recently, this effect was directly observed in experiments.[45]

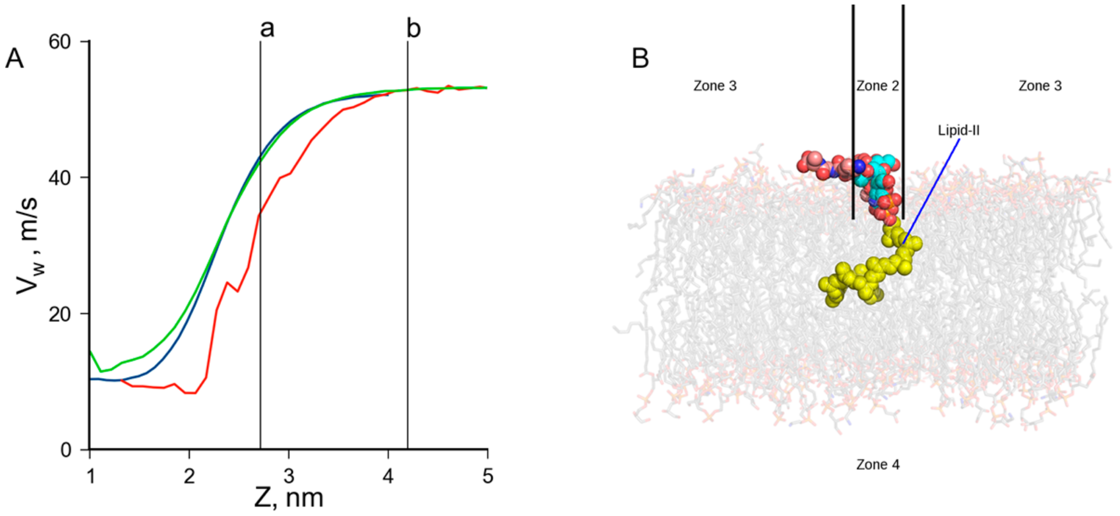

Figure 8. (A) The average absolute velocity (v_w) of water in the POPG/POPE 3:1 bilayer plotted as a function of the distance from the bilayer center (z). The middle of the bilayer corresponds to $z = 0.0$ nm. The results are given for bilayers with (red and green lines) and without (blue line) an inserted lipid-II molecule. For the system with lipid-II: red line, solvent region above the polar head of the lipid-II (zone-2, see text); green line, solvent region zone-3. The boundaries of the "transitional zone" for water (see text) are indicated with vertical lines marked "a" and "b". (B) Side view of the POPG/POPE bilayer (thin gray lines) with the immersed lipid-II molecule (shown in ball presentation). The water molecules are omitted for clarity. The boundaries of the solvent zone-2 (see text) are indicated with vertical lines. Zones 3 and 4 are also shown.

Therefore, in the zone $|z| < 0.7$ nm, water is losing its natural packing and single "travelling waters" appear.

The Effect of Local Perturbations of the Lipid Bilayer on Water Dynamics. While this manuscript was in preparation, new important experimental data characterizing translational hydration dynamics within 0.5−1.5 nm of the surface of various PC-based liposomes was published.[46,47] These results were obtained using the recently developed Overhauser dynamic nuclear polarization (ODNP) technique. For the first time, it was concluded that there is a strong decoupling of the surface and bulk water dynamics, which may prove important to the function of biomolecular systems in cellular environments. This fundamental observation can be directly used to assess the reliability of the atomistic simulations presented in this work. To do this, we decided to take the system "lipid-II in the model bacterial membrane composed of POPG and POPE lipids". Recently, we demonstrated[48] that the embedding of lipid-II into such a bilayer induces prominent local (<1 nm size) perturbations of the membrane due to high-amplitude moves of its hydrophobic tail, strong interactions of its polar head with surrounding lipids, and specific structural/dynamic properties of the bilayer. Therefore, the POPG/POPE membrane with and without an inserted lipid-II molecule represents a suitable test case to address the question mentioned above.

The behavior of water molecules was analyzed in four regions: (1) near both surfaces of the pure bilayer; (2) in the cylindrical volume above the polar head of the lipid-II (see Materials and Methods); (3) in the remaining volume of the simulation box, on the same side as in case 2; and (4) near the bilayer surface, on the opposite side with respect to the lipid-II polar head. The corresponding zones are referred to as zones 1−4. The calculated distribution of $v_w(z)$ is shown in Figure 8A. As it was reasonable to expect, the presence of the polar head of the lipid-II, which towers above the membrane surface by ∼0.3−0.4 nm,[48] disturbs the density of waters in zone-2, at 1.5 nm $< |z| <$ 2.2 nm (data not shown). In contrast, the characteristics of water in zones 3 and 4 are very similar to those in an unperturbed lipid bilayer (without lipid-II). We should note that even in zone-2 water "feels" the presence of the lipid-II very locally; the density curve reaches a plateau simultaneously with zones 1, 3, 4 at $|z| =$ 2.72 nm. At the same time, the corresponding velocity plots for zone-2 are drastically different from the others (Figure 8A).

But the most striking result is that in all zones 1−4 the average absolute velocity plots ($v_w(z)$) reach their constant values (inherent in the bulk solvent) at the same distance from the bilayer center: $|z| = 4.2$ nm. In other words, even strong perturbations in close proximity to the bilayer surface do not affect the dynamics of the bulk water; all differences are localized in the "transitional zone", which serves as a peculiar "buffer" between the membrane interface and the free solution. This strongly supports the conclusion made in experimental work[47] about the decoupling of interfacial and bulk water properties. Also, this validates the computational approach developed here.

Lessons from Studies of Water Dynamics in Membranes. Some methodological issues can be formulated based on this study. First, the amount of water in the MD box should be high enough to ensure bulk solvent conditions on its edges. Here, this was realized in the DOPC bilayer (120 waters per lipid), where the thickness of the water layer on both sides was *ca.* 6.0 nm. The minimal distance from the waterless nonpolar core to the box edge should be ≈3.15 nm, which is required for water to reach its bulk properties. Other systems were constructed with a smaller hydration degree (Table S2), where the thickness of the water layers was already close to the lower limit. Second, as discussed above, switching to polarizable force fields does not change the principal conclusions made, at least for such an important characteristics as the free energy profile. So, the current force fields seem to be adequate for capturing the main tendencies of water dynamics in membranes.

Furthermore, as demonstrated above, a number of small but fundamental effects, such as the spontaneous insertion of individual water molecules into the hydrophobic membrane region, can explain some important aspects of the biomembrane's functional dynamics. According to their nature, such phenomena are determined by local fluctuations in lipid/water systems and can be "trapped" only in atomistic simulations. They cannot be correctly described in the framework of continuum models only, even if they perfectly reproduce the available macroscopic experimental data.

We should emphasize that a detailed analysis of water behavior in the presence of lipid bilayers was possible because we did not impose any constraints onto the simulations. Although this seriously limited the conformational sampling of water in the hydrophobic membrane interior, the availability of long MD trajectories ensured sufficient statistics of the described "events". Moreover, unconstrained atomistic simulations allowed for the analysis of the intimate fluctuation-dependent phenomena described above. Obviously, all such details would have been unavailable if some artificial constraints were imposed.

CONCLUSIONS

Long-term MD simulations of several hydrated lipid bilayers containing some 300 lipids and (1−3) × 10^5 waters provided interesting atomistic details of water dynamics near the membrane surface and in its hydrophobic interior. As it was reasonable to expect, in all cases water drastically changes its dynamic behavior when moving from the bulk solution and approaching the bilayer interface. Thus, the average absolute velocity of water continuously drops and reaches quite a deep (∼35 m/s) minimum in the vicinity of strong water binders, phosphates, carbonyls, and (in PC-bilayers) trimethyl ammonium groups of lipids. Here, water molecules form H-bonds with the latter, thus slowing down and losing kinetic energy. At smaller distances from the bilayer center, the velocities grow and can exceed those in the bulk region. This is also reflected in an increase of the local diffusion coefficient toward the middle plane of the membrane, a fact observed previously in some[13,22] but not all[16] studies. Apart from the velocities, another important characteristic of water behavior is its ability to form H-bonds with its neighbors. The penetration of waters into the membrane's nonpolar zones is accompanied by a decline in the total number of H-bonds and a replacement of water−water hydrogen bonds by the stronger water−lipid ones.

Accordingly, the overall picture of water diffusivity agrees well with numerous experimental and computational results obtained earlier. At the same time, a number of interesting and biologically relevant details observed in this work have not been reported or not sufficiently discussed yet in the literature. Thus, water molecules "sense" the presence of the membrane unexpectedly early, before water density begins to decrease. In this "transitional zone", average velocity distributions of waters and their H-bonding patterns deviate from those in the bulk solution, although some other important structural and dynamic characteristics (radial distribution functions, lifetimes of H-bonds) do not change so much. Unexpectedly, the upper (closest to bulk water) boundary of such a transitional zone does not depend on strong local perturbations of the lipid bilayer. This agrees perfectly with very recent experimental observations[46,47] and proves the decoupling between the surface and bulk water. Also, near the membrane surface and in the polar group region water movements become anisotropic; solvent molecules preferentially move outward from the bilayer center. This simulation result is confirmed by neutron scattering data.[49] This effect increases at smaller $|z|$ and becomes too noisy in the middle of the membrane.

Moreover, inside the membrane, water movements exhibit large-scale fluctuations, because of a much smaller concentration (and, therefore poor statistics) and the stochastic nature of their hydrophobic microenvironment. Long-term MD simulations allowed for the observation of a number of rare and extremely interesting events, namely, the spontaneous penetration of single water molecules into the hydrophobic zone of acyl chains of lipids. On average, 1 time per *ca.* 2−3 ns the water molecule even crosses the central plane of the membrane. Roughly, two types of such "events" were delineated, fast (∼ 50 ps) and relatively slow (up to 750 ps) ones (see above). In these cases, single water molecules can acquire anomalously high velocities and rapidly change the directions of their movements, depending on their nearest lipid neighbors. This results in strong fluctuations of the mass and electric field created by water dipole in an environment with low dielectric permeability. Here, water molecules demonstrate a dramatic weakening of their interactions with neighbors; they have neither H-bonded partners nor other polar groups with which to establish energetically favorable contacts. That is why their high speed movements help minimize their residence time in this "alien" medium.

Despite the fact that the exact details of fast water diffusion in the middle part of membranes depend on the physicochemical properties of the latter (lipid composition, hydration degree, presence of ions, and so on), at least for four simulated systems the picture of water diffusivity looks quite similar. This allows to establish a proposal about the universal character of such phenomena in cell membranes. On the other hand, water dynamics in the presence of an artificial "membrane", a cyclohexane layer separating two water reservoirs, reveals a number of principal differences with respect to lipid bilayers. The most striking of them are the much less efficient braking of waters near the slab boundaries and the different H-bonding picture. Thus, although a layer of small apolar organic molecules separates the opposite water volumes well, like lipid bilayers do, this "membrane" is much more permeable to water. Also, in contrast to lipids, such a system has no means for a fine-tuned regulation of water dynamics, which is necessary for many cell processes.

What might be the biological relevance of the nontrivial behavior of water in cell membranes? In our opinion, one of the most significant results of this work is the description of the spontaneous penetration of single waters into the hydrophobic core. Although such events occur relatively rarely, this seems to be sufficient to create in globally equilibrated lipid bilayers microscopic "defects" or "hot spots", which locally destabilize the lipid bilayers in their central parts. In other words, in native-like membranes there is a co-existence of a "quiet" interfacial and a local perturbed central zone. One may speculate that such a heterogeneity plays a dual role: it helps to maintain the overall integrity of the membrane, while also carrying a germ of instability, which is required for adaptation processes. In the latter case, this facilitates many more global membrane perturbations induced by the binding/insertion of external agents (proteins, peptides, and so on) and/or action of such factors as transmembrane voltage, pressure/temperature changes, and other.[50,51]

It seems that there is no direct relationship between the overall structural (area per lipid, thickness, *etc.*) and dynamic (order parameters of acyl chains) properties of lipid bilayers and the ability of water molecules to penetrate spontaneously deep into the membrane core, to gain very high velocities there, and to cross the hydrophobic barrier. At the same time, the nature of the bilayer can play a critical role in water behavior. We hypothesize that the anomalous properties of water in the central part of lipid membranes are determined by point fluctuations. The latter ones, in turn, are caused by a complex interplay of different factors, and most of them are yet to be delineated. At present, such phenomena can be efficiently studied with the help of atomic-scale computational experiments.

MATERIALS AND METHODS

MD Simulations. The MD simulations were carried out with the GROMACS version 4.0.4 program[52] for symmetric (according to composition of monolayers) hydrated DOPC, DPPC, DOPC/DPPC (9:1), and DOPS bilayers containing 288 lipid molecules (144 per leaflet), as well as for explicit water-cyclohexane-water system and a box with explicit water (Table S2). The MD trajectories for the aforementioned systems were either taken from our previous studies,[7,25,26] or just recalculated at larger time scales using similar computational protocols. The details of the MD simulations are given in the Supporting Information. The MD data for the POPG/POPE 3:1 bilayer with and without an inserted lipid-II molecule were taken from Chugunov *et al.*[48] Related simulation details can also be found there.

Processing of MD Trajectories: Water Dynamics. The MD trajectories were analyzed with the help of the original software and modified GROMACS utilities. This was done for near-equilibrium parts ($\geq$10 ns) of the trajectories. At least 100 MD frames were taken for the analysis with an interval $\Delta t = 10$ ps. To assess the properties of water at different distances from the bilayer center, the simulated boxes were subdivided into a number of layers perpendicular to the bilayer normal, axis *Z*. In the MD frame *k*, the thickness (h_k) of each layer was equal to $h_k = L^k_{\text{box}}/N_{\text{l}}$, where L^k_{box} is the size of the box along *Z*, and N_{l} is the number of layers. Upon construction of the plots, the value of L_{box} averaged over the MD trajectory was used (Table S2). In all cases, N_{l} was equal to 100. The value $z = 0$ was attributed to the bilayer center. (Unless otherwise indicated, similar coordinate system and analysis protocol were also used for the water-cyclohexane-water box, where the *Z*-axis was chosen perpendicular to the plane defining water−cyclohexane interface.) Water regions in the simulation box with the POPG/POPE 3:1 bilayer with an immersed lipid-II molecule were defined as follows. Zone-2 region was defined as a cylinder of radius 0.5 nm with its axis parallel to the bilayer normal (z) and centered on the atoms of the lipid-II polar headgroup (Figure 8B).

The following average parameters related to structural and dynamic properties of water were considered: the velocity (absolute value (v_{w}), projection on *Z*-axis (v_z), angle with *Z*-axis (α)); the density (ρ_{w}); the number of H-bonds per water molecule (n_{Hbn}); the lifetime of the H-bond (τ_{Hbn}); the coefficient of local diffusion (D_{w}). The corresponding distributions along the *Z*-axis were obtained as follows. First, for each particular value of z_i, the property was calculated by averaging over the water molecules found in layer $[z_i, z_{i+1}]$ with thickness h_k in the MD frame *k*. Then, an averaging over all the considered MD frames was performed. The absolute velocity of water *j* in frame *k* was calculated as: $\vec{v}_{jk} = (\vec{r}_{jk+1} - \vec{r}_{jk})/\mathrm{d}t$, where $\vec{r}_{jk}$ is the radius-vector of the center of mass (CM) of water *j*. We should note that because of such a diffusion-based treatment of velocities, their values depend on Δt. Therefore, the latter parameter should be chosen with care. At the same time, the current value of $\Delta t = 10$ ps seems to be quite a reasonable choice as it allows for a detailed treatment of all the dynamic parameters studied in this work and is comparable with the characteristic time scale of the phenomena in question (see, also ref 22 for more details). Finally, the employment of different values of Δt gives similar *z*-dependencies of water dynamics and therefore does not change the conclusions made in this study (data not shown). The lifetime of an H-bond was determined as the time interval of its persistent observation in the MD. For a given value z_i, H-bonds with *z*-coordinates of the centers of the segments connecting the donor and acceptor atoms located in the layer $[z_i, z_{i+1}]$ were taken into account.

The following scheme of data averaging was used to assess the statistical errors of v_{w} shown in Figure 1. The MD trajectory of 200 ns length was subdivided into 10 successive parts. For each part, the values of v_w were calculated as described above. Then, the mean and standard deviation were calculated.

The local diffusion coefficient of water (D_w) was estimated as described in previously[22,53] (see also the Supporting Information). The potential of the mean force for water penetration into the bilayer core was determined from the water density ($\rho_w(z)$) profiles. Because all water layers have the same volume, the corresponding free energy of transfer can be written as follows: $dG = -kT \ln(\rho_w(z_i)/\rho_w(0)$, where $\rho_w(0)$ is the density of the bulk water. Taking into account that the average frequency of spontaneous water penetration inside the bilayer core with $|z| < 0.5$ nm exceeds 0.30 ns^{-1} (see Table S1), the average water density here is not equal to zero, thus allowing for the statistical treatment of the data.

Statistics of "Events": The Spontaneous Penetration of Water into the Membrane Core. The term "event" was used to define the cases of water detection near the bilayer center, with coordinates $|z| \leq z_{\text{core}}$. The events were considered during the time period when a particular water molecule was continuously observed in this region. Two values of z_{core} were employed: 0.5 and 0.7 nm. The first of them corresponds to the region where the density of water reaches zero (within a 1% error), while the second one indicates the boundary where strong fluctuations of water velocities appear. For each event, the following parameters were evaluated: beginning/termination/duration times (t_1, t_2, $\tau = t_2 - t_1$); average z coordinate, the absolute velocity (v_w) and its z-component (v_z); the mean x/y coordinates of water CM; the average number of neighboring waters within 0.5 nm; the average number of H-bonds with other water molecules. Two additional characteristics were also registered for each event: the indicators of water crossing the central plane with $z = 0$ and its escape on the same or opposite sides of the membrane.

Conflict of Interest: The authors declare no competing financial interest.

Supporting Information Available: A table with event statistics, the MD-simulation protocol, a table with characteristics of the studied systems, a figure with density profiles, a figure with reduced statistics data, a figure with the average absolute velocity of water, a figure with two-dimensional histograms of the average velocities distribution of water molecules over their absolute values and orientation, a figure with the average local diffusion coefficient, a figure with the excess free energy profile of water, a figure with the average number of H-bonds per water molecule, a figure with the average lifetime of H-bonds per water molecule, a figure with the anisotropy of water moves in cyclohexane slab, a figure with a pair of water molecules traveling through the central hydrophobic core of DOPC bilayer. This material is available free of charge *via* the Internet at http://pubs.acs.org.

Acknowledgment. Authors thank Darya Pyrkova, Dmitry Nolde and Anton Chugunov for providing most of the MD trajectories. Force field parameters for the cyclohexane were generously provided by Dr. Pavel Volynsky. Access to computational facilities of the Joint Supercomputer Center RAS (Moscow) and the Moscow Institute of Physics and Technology is gratefully acknowledged. We thank Ms. Anastasia Efremova for editing the manuscript. This work was supported by the Ministry of Education and Science of the Russian Federation (State contract 14.514.11.4069), by the Russian Foundation for Basic Research and by the RAS Programmes "Basic fundamental research for nanotechnologies and nanomaterials" and "Molecular and cellular biology".

REFERENCES AND NOTES

1. Marguet, D.; Lenne, P.-F.; Herve, R.; He, H.-T. Dynamics in the Plasma Membrane: How to Combine Fluidity and Order. *EMBO J.* **2006**, *25*, 3446–3457.
2. Bagatolli, L.; Ipsen, J.; Simonsen, A.; Mouritsen, O. An Outlook on Organization of Lipids in Membranes: Searching for a Realistic Connection with the Organization of Biological Membranes. *Prog. Lipid Res.* **2010**, *49*, 378–389.
3. Jorgensen, K.; Mouritsen, O. Phase Separation Dynamics and Lateral Organization of Two-Component Lipid Membranes. *Biophys. J.* **1995**, *69*, 942–954.
4. Lingwood, D.; Simons, K. Lipid Rafts as a Membrane-Organizing Principle. *Science* **2010**, *327*, 46–50.
5. Brown, D.; London, E. Structure and Origin of Ordered Lipid Domains in Biological Membranes. *J. Membr. Biol.* **1998**, *164*, 103–114.
6. Faller, R.; Marrink, S. Simulation of Domain Formation in DLPC-DSPC Mixed Bilayers. *Langmuir* **2004**, *20*, 7686–7693.
7. Pyrkova, D.; Tarasova, N.; Pyrkov, T.; Krylov, N.; Efremov, R. Atomic-Scale Lateral Heterogeneity and Dynamics of Two-Component Lipid Bilayers Composed of Saturated and Unsaturated Phosphatidylcholines. *Soft Matter* **2011**, *7*, 2569–2579.
8. Disalvo, E.; Lairion, F.; Martini, F.; Tymczyszyn, E.; Frías, M.; Almaleck, H.; Gordillo, G. Structural and Functional Properties of Hydration and Confined Water in Membrane Interfaces. *J. Biochim. Biophys. Acta* **2008**, *1778*, 2655–2670.
9. Gennis, R. *Biomembranes. Molecular Structure and Function*; Springer: New York, 1989.
10. Bagchi, B. Water Dynamics in the Hydration Layer around Proteins and Micelles. *Chem. Rev.* **2005**, *105*, 3197–3219.
11. Debnath, A.; Mukherjee, B.; Ayappa, K.; Maiti, P.; Lin, S.-T. Entropy and Dynamics of Water in Hydration Layers of a Bilayer. *J. Chem. Phys.* **2010**, *133*, 174704.
12. Kausik, R.; Han, S. Dynamics and State of Lipid Bilayer-Internal Water Unraveled with Solution State ^{1}H Dynamic Nuclear Polarization. *Phys. Chem. Chem. Phys.* **2011**, *13*, 7732–7746.
13. Marrink, S.; Berendsen, H. Simulation of Water Transport through a Lipid Membrane. *J. Phys. Chem.* **1994**, *98*, 4155–4168.
14. Rosso, L.; Gould, I. Structure and Dynamics of Phospholipid Bilayers Using Recently Developed General All-Atom Force Fields. *J. Comput. Chem.* **2008**, *29*, 24–37.
15. Nagle, J.; Mathai, J.; Zeidel, M.; Tristram-Nagle, S. Theory of Passive Permeability through Lipid Bilayers. *J. Gen. Physiol.* **2008**, *131*, 77–85.
16. Bhide, S.; Berkowitz, M. Structure and Dynamics of Water at the Interface with Phospholipid Bilayers. *J. Chem. Phys.* **2005**, *123*, 224702.
17. Zhao, W.; Moilanen, D.; Fenn, E.; Fayer, M. Water at the Surfaces of Aligned Phospholipid Multibilayer Model Membranes Probed with Ultrafast Vibrational Spectroscopy. *J. Am. Chem. Soc.* **2008**, *130*, 13927–13937.
18. Nagle, J.; Tristram-Nagle, S. Structure of Lipid Bilayers. *Biochim. Biophys. Acta* **2000**, *1469*, 159–195.
19. Damodaran, K.; Merz, J. Head Group–Water Interactions in Lipid Bilayers: A Comparison between DMPC and DLPE Based Lipid Bilayers. *Langmuir* **1993**, *9*, 1179–1183.
20. Pasenkiewicz-Gierula, M.; Takaoka, Y.; Miyagawa, H.; Kitamura, K.; Kusumi, A. Rotational Motion of Square Planar Copper Complexes in Solution and Phospholipid Bilayer Membrane. *J. Phys. Chem. A* **1997**, *101*, 5596–5606.
21. Fukuma, T.; Higgins, M.; Jarvis, S. Direct Imaging of Individual Intrinsic Hydration Layers on Lipid Bilayers at Angstrom Resolution. *Biophys. J.* **2007**, *92*, 3603–3609.
22. Shinoda, W.; Mikami, M.; Baba, T.; Hato, M. Molecular Dynamics Study on the Effects of Chain Branching on the Physical Properties of Lipid Bilayers. 2. Permeability. *J. Phys. Chem. B* **2004**, *108*, 9346–9356.
23. Breukink, E.; de Kruijff, B. Lipid II as a Target for Antibiotics. *Nat. Rev. Drug Discovery* **2006**, *5*, 321–332.
24. Polyansky, A.; Volynsky, P. E.; Nolde, D. E.; Arseniev, A. S.; Efremov, R. G. The Role of Lipid Charge in Organization of Water/Lipid Bilayer Interface: Insights *via* Computer Simulations. *J. Phys. Chem. B* **2005**, *109*, 15052–15059.
25. Pyrkova, D.; Tarasova, N.; Pyrkov, T.; Krylov, N.; Efremov, R. Lateral Clustering of Lipids in Hydrated Bilayers Composed of Dioleoylphosphatidylcholine and Dipalmitoylphosphatidylcholine. *Biol. Membrany* **2011**, *28*, 298–306.
26. Pyrkova, D.; Tarasova, N.; Krylov, N.; Nolde, D.; Pentkovsky, V.; Efremov, R. Dynamic Clustering of Lipids in Hydrated Two-Component Membranes: Results of Computer Modeling and Putative Biological Impact. *J. Biomol. Struct. Dyn.* **2013**, *31*, 87–95.

27. Berkowitz, M.; Vacha, R. Aqueous Solutions at the Interface with Phospholipid Bilayers. *Acc. Chem. Res.* **2012**, *45*, 74–82.
28. Jansen, M.; Blume, A. A Comparative Study of Diffusive and Osmotic Water Permeation Across Bilayers Composed of Phospholipids with Different Head Groups and Fatty Acyl Chains. *Biophys. J.* **1995**, *68*, 997–1008.
29. Huster, D.; Jin, A.; Arnold, K.; Gawrisch, K. Water Permeability of Polyunsaturated Lipid Membranes Measured by ^{17}O NMR. *Biophys. J.* **1997**, *73*, 855–864.
30. Mathai, J.; Tristram-Nagle, S.; Nagle, J.; Zeidel, M. Structural Determinants of Water Permeability through the Lipid Membrane. *J. Gen. Physiol.* **2008**, *131*, 69–76.
31. Finkelstein, A. *Water Movement through Lipid Bilayer, Pores and Plasma Membranes*; Wiley-Interscience: New York, 1987.
32. Gawrisch, K.; Gaede, H.; Mihailescu, M.; White, S. Hydration of POPC Bilayers Studied by ^{1}H-PFG-MAS-NOESY and Neutron Diffraction. *Eur. Biophys. J.* **2007**, *36*, 281–291.
33. Bauer, B.; Lucas, T.; Meninger, D.; Patel, S. Water Permeation through DMPC Lipid Bilayers Using Polarizable Charge Equilibration Force Fields. *Chem. Phys. Lett.* **2011**, *508*, 289–294.
34. Finkelstein, A. Water and Nonelectrolyte Permeability of Lipid Bilayer Membranes. *J. Gen. Physiol.* **1976**, *68*, 127–135.
35. Bemporad, D.; Luttmann, C.; Essex, J. Behaviour of Small Solutes and Large Drugs in a Lipid Bilayer from Computer Simulations. *Biochim. Biophys. Acta* **2005**, *1718*, 1–21.
36. Pandey, P.; Roy, S. Headgroup Mediated Water Insertion into the DPPC Bilayer: A Molecular Dynamics Study. *J. Phys. Chem. B* **2011**, *115*, 3155–3163.
37. Marrink, S.; Jahnig, F.; Berendsen, H. Proton Transport Across Transient Single-File Water Pores in a Lipid Membrane Studied by Molecular Dynamics Simulations. *Biophys. J.* **1996**, *71*, 632–647.
38. Tepper, H.; Voth, G. Mechanisms of Passive Ion Permeation through Lipid Bilayers: Insights from Simulations. *J. Phys. Chem. B* **2006**, *110*, 21327–21337.
39. Kucerka, N.; Nagle, J.; Sachs, J.; Feller, S.; Pencer, J.; Jackson, A.; Katsaras, J. Lipid Bilayer Structure Determined by the Simultaneous Analysis of Neutron and X-ray Scattering Data. *Biophys. J.* **2008**, *95*, 2356–2367.
40. Petrache, H.; Tristram-Nagle, S.; Gawrisch, K.; Harries, D.; Parsegian, V.; Nagle, J. Structure and Fluctuations of Charged Phosphatidylserine Bilayers in the Absence of Salt. *Biophys. J.* **2004**, *86*, 1574–1586.
41. Polyansky, A.; Volynsky, P.; Arseniev, A.; Efremov, R. Adaptation of a Membrane Active Peptide to Heterogeneous Environment. I. Structural Plasticity of the Peptide. *J. Phys. Chem. B* **2009**, *113*, 1107–1119.
42. Polyansky, A.; Volynsky, P.; Arseniev, A.; Efremov, R. Adaptation of a Membrane Active Peptide to Heterogeneous Environment. II. The Role of Mosaic Nature of the Membrane Surface. *J. Phys. Chem. B.* **2009**, *113*, 1120–1126.
43. Volke, F.; Eisenblatter, S.; Galle, J.; Klose, G. Dynamic Properties of Water at Phosphatidylcholine Lipid-Bilayer Surfaces as Seen by Deuterium and Pulsed Field Gradient Proton NMR. *Chem. Phys. Lipids* **1994**, *70*, 121–131.
44. Venable, R.; Pastor, R. Molecular Dynamics Simulations of Water Wires and Water/Octane Model Systems. *J. Chem. Phys.* **2002**, *116*, 2663–2664.
45. Piatkowski, L.; de Heij, J.; Bakker, H. J. Probing the Distribution of Water Molecules Hydrating Lipid Membranes with Ultrafast Förster Vibrational Energy Transfer. *J. Phys. Chem. B* **2013**, *117*, 1367–1377.
46. Cheng, C.-Y.; Wang, J.-Y.; Kausik, R.; Lee, K. Y. C. An Ultrasensitive Tool Exploiting Hydration Dynamics to Decipher Weak Lipid Membrane-Polymer Interactions. *J. Magn. Reson.* **2012**, *215*, 115–119.
47. Frank, J. M.; Scott, J. A.; Han, S. Nonlinear Scaling of Surface Water Diffusion with Bulk Water Viscosity of Crowded Solutions. *J. Am. Chem. Soc.* **2013**, *135*, 4175–4178.
48. Chugunov, A. O.; Pyrkova, D. V.; Nolde, D. E.; Polyansky, A. A.; Pentkovsky, V. M.; Efremov, R. G. Lipid-II Forms Potential “Landing Terrain” for Lantibiotics in Simulated Bacterial Membrane. *Sci. Rep.* **2013**, *3*, 1678.
49. Russo, D.; Murarka, R. K.; Copley, J. R. D.; Head-Gordon, T. Molecular View of Water Dynamics near Model Peptides. *J. Phys. Chem. B* **2005**, *109*, 12966–12975.
50. Gurtovenko, A.; Anwar, J.; Vattulainen, I. Defect-Mediated Trafficking across Cell Membranes: Insights from *in Silico* Modeling. *Chem. Rev.* **2010**, *110*, 6077–6103.
51. Marrink, S.; de Vries, A.; Tieleman, D. Lipids on the Move: Simulations of Membrane Pores, Domains, Stalks and Curves. *Biochim. Biophys. Acta* **2009**, *1788*, 149–168.
52. Hess, B.; Kutzner, C.; van der Spoel, D.; Lindahl, E. Algorithms for Highly Efficient, Load-Balanced, and Scalable Molecular Simulation. *J. Chem. Theory Comput.* **2008**, *4*, 435–447.
53. Roark, M.; Feller, S. Molecular Dynamics Simulation Study of Correlated Motions in Phospholipid Bilayer. *J. Phys. Chem. B* **2009**, *113*, 13229–13234.